

[Click here to view linked References](#)

1
2
3
4 1 **Niche differences in co-occurring cryptic coral species (*Pocillopora* spp.)**
5
6
7
8
9
10
11

12 4 Erika C. Johnston^{1*}, Alex S. J. Wyatt², James J. Leichter³, Scott C. Burgess¹
13
14
15
16
17 6 *corresponding author: ejohnston@bio.fsu.edu
18
19 7 ¹ Department of Biological Science, Florida State University, 319 Stadium Drive, Tallahassee,
20
21 8 FL, 32306-4296, USA.
22
23
24 9 ² Department of Ocean Science and Hong Kong Branch of the Southern Marine Science and
25
26 10 Engineering Guangdong Laboratory (Gunagzhou), The Hong Kong University of Science and
27
28 11 Technology, Clear Water Bay, Kowloon, Hong Kong, China.
29
30
31 12 ³ Scripps Institution of Oceanography, University of California San Diego, La Jolla, CA, USA.
32
33
34 13
35
36 14
37
38
39
40
41
42
43
44
45
46
47
48
49
50
51
52
53
54
55
56
57
58
59
60
61
62
63
64
65

1
2
3
4 15 **Abstract**
5
6
7 16 Cryptic species that are morphologically similar co-occur because either the rate of competitive
8
9 17 exclusion is very slow, or because they are not, in fact, ecologically similar. The processes that
10
11 18 maintain cryptic local diversity may, therefore, be particularly subtle and difficult to identify.
12
13
14 19 Here, we uncover differences among several cryptic species in their relative abundance across a
15
16 20 depth gradient within a dominant and ecologically important genus of hard coral, *Pocillopora*.
17
18
19 21 From extensive sampling unbiased towards morphological characters, at multiple depths on the
20
21 22 fore reef around the island of Mo'orea, French Polynesia, we genetically identified 673 colonies
22
23 23 in the *Pocillopora* species complex. We identified 14 mitochondrial Open Reading Frame
24
25 24 haplotypes (mtORFs, a well-studied and informative species marker used for pocilloporids),
26
27 25 which included at least six nominal species, and uncovered differences among haplotypes in their
28
29 26 relative abundance at 5, 10, and 20 m at four sites around the island. Differences in relative
30
31 27 haplotype abundance across depths were greater than differences among sites separated by
32
33 28 several kilometers. The four most abundant species are often visibly indistinguishable at the
34
35 29 gross colony level, yet they exhibited stark differences in their associations with light irradiance
36
37 30 and daily water temperature variance. The pattern of community composition was associated
38
39 31 with frequent cooling in deeper versus shallower water more than warmer temperatures in
40
41 32 shallow water. Our results indicate that these cryptic species are not all ecologically similar. The
42
43 33 differential abundance of *Pocillopora* cryptic species across depth should promote their
44
45 34 coexistence at the reef scale, as well as promote resilience through response diversity.
46
47
48 35
49
50
51
52
53
54
55 36 Keywords: Depth, internal waves, niche partitioning, Mo'orea, temperature variance
56
57
58
59
60
61
62
63
64
65

1
2
3
4 37 **Introduction**
5
6
7 38 Understanding the mechanisms that give rise to, and maintain, biodiversity allows for
8
9 39 better predictions of how communities respond to natural and anthropogenic disturbance (Levin
10
11 40 and Lubchenco 2008). Molecular phylogenetic studies frequently identify the co-occurrence of
12
13 41 cryptic species (Bickford et al. 2007; Bongaerts et al. 2021), which would not be expected to
14
15 42 coexist if they were truly ecologically similar and competing for the same limiting resource
16
17 43 (Zhang et al. 2004; McPeek and Gomulkiewicz 2005). Studying co-occurring cryptic species
18
19 44 provides the opportunity to discover biological differences among cryptic species beyond
20
21 45 morphological characters, and how such differences arise and influence community response to
22
23 46 environmental change.

24
25
26
27
28 47 Niche partitioning among cryptic species may be particularly subtle, and difficult to
29
30
31 48 identify in natural communities. Much of the theory of species coexistence is based on
32
33 49 competition, where species coexist via the relative strength of two fundamental classes of
34
35 50 mechanisms (Chesson 2000): equalizing and stabilizing processes. Processes that equalize
36
37 51 frequency-independent fitness differences between species slow competitive exclusion.

38
39
40 52 Compared to non-cryptic species, cryptic species are likely to be ecologically more similar, so
41
42 53 may co-occur simply because the rate of competitive exclusion is slow enough to permit them to
43
44 54 persist for substantial periods of time before one species eventually dominates (McPeek and
45
46 55 Gomulkiewicz 2005). Species coexist in the long-term due to stabilizing processes, where
47
48 56 competition causes species to limit themselves more than their competitors (i.e., intraspecific
49
50 57 competition > interspecific competition). Niche, or resource, partitioning is an important and
51
52 58 common stabilizing mechanism (Chesson 2000), in addition to asynchronous fluctuations in
53
54 59 population dynamics (Snyder and Chesson 2004), environmental fluctuations (De Meester et al.

1
2
3
4 60 2011; Montero-Pau et al. 2011), differences in dispersal (Berkley et al. 2010; Bode et al. 2011;
5
6 61 Boulay et al. 2014; Daly et al. 2021) and density-dependent mate competition (Levitin 2004;
7
8 62 Zhang et al. 2004). Importantly, equalizing effects modify the magnitude of stabilizing effects
9
10 63 needed for coexistence. If cryptic species, being morphologically indistinguishable, are
11
12 64 ecologically similar, there will be smaller fitness differences between them and less niche
13
14 65 partitioning will be required to promote their coexistence (Mayfield and Levine 2010). Thus,
15
16 66 only very subtle niche differences among cryptic species are required for their coexistence.
17
18
19
20
21 67 Scleractinian corals, the foundation species that build diverse coral reefs, are notorious
22
23 68 for containing high species diversity and cryptic species (Knowlton et al. 1992; Pinzón et al.
24
25 69 2013; Schmidt-Roach et al. 2013; Richards et al. 2016; Gélin et al. 2017; Bongaerts et al. 2021;
26
27 70 Prada and Hellberg 2021). Explanations for why such species commonly co-occur at fine scales,
28
29 71 such as on the same reef, remain elusive. Part of the problem is that the few studies on cryptic
30
31 72 species distribution have focused mostly on one morphological type across environmental
32
33 73 gradients (e.g., Levitan et al. 2011, Warner et al. 2015, De Palmas et al. 2018, Johnston et al.
34
35 74 2018). However, the highly plastic morphology exhibited by scleractinians allows species to
36
37 75 modify their skeletal structure in response to changes in environmental conditions (Todd 2008),
38
39 76 which allows genetically identified species to shift between morphospecies (Paz-García et al.
40
41 77 2015a). That is, while a morphological species can contain multiple genetic species (Edmunds et
42
43 78 al. 2016; De Palmas et al. 2018), individuals from the same genetic species can also look like
44
45 79 individuals from different morphological species (Pinzón et al. 2013; Martí-Puig et al. 2014;
46
47 80 Paz-García et al. 2015a; Edmunds et al. 2016; Gómez- Corrales and Prada 2020). Thus, studying
48
49 81 the co-occurrence of cryptic species across environmental gradients requires that samples
50
51 82 collected for genetic analysis in order to identify species be sampled without regards to
52
53
54
55
56
57
58
59
60
61
62
63
64
65

1
2
3
4 83 morphology. Furthermore, environmental gradients across depths in particular, are hypothesized
5
6 84 to be an important factor causing divergence among scleractinian cryptic marine species
7
8 85 (Knowlton et al. 1992; Prada and Hellberg 2021).
9
10

11 86 At Mo'orea, French Polynesia, *Pocillopora* colonies dominate the fore reef substratum,
12
13 87 and multiple morphologies commonly co-occur and include both geographically widespread and
14
15 88 endemic species (Forsman et al. 2013). *Pocillopora* species on the fore reef are all species that
16
17 89 are considered to reproduce via broadcast spawning (Bouwmeester et al. 2011; Schmidt-Roach et
18
19 90 al. 2012). The brooding species, *P. damicornis* and *P. acuta*, have not been seen or sampled on
20
21 the fore reef of Mo'orea (Burgess et al. 2021). Gross colony morphology is an unreliable
22
23 91 indicator of species (Martí-Puig et al. 2014; Paz-García et al. 2015b), but species can be
24
25 92 identified genetically (Flot et al. 2008; Schmidt-Roach et al. 2014; Gélin et al., 2017; Johnston et
26
27 93 al. 2017).
28
29 94 al. 2017).

30
31 95 The near complete loss of live coral (<5% cover at all fore reef sites around Mo'orea)
32
33 96 after several major disturbances ending in 2010 (Adam et al. 2011), and subsequently high
34
35 97 *Pocillopora* recruitment and colony growth into vacant space in the following years (Tsounis and
36
37 98 Edmunds 2016), provides a unique context with which to examine the role of depth in structuring
38
39 99 *Pocillopora* community composition because observed abundance patterns nine years later will
40
41 100 reflect the net outcomes of recruitment, growth, and survival, and not differences in disturbance
42
43 101 history. Our goals were to: 1) sample *Pocillopora* without regards to morphology and quantify
44
45 102 the relative abundance of cryptic genetic lineages across depths at multiple sites on the fore reef
46
47 103 around Mo'orea, and 2) identify the relative contribution of different aspects of the temperature
48
49 104 and light regimes in potentially explaining differences in community composition across depths
50
51 105 and sites. We hypothesized that the relative abundance of cryptic species would differ across
52
53
54
55
56
57
58
59
60
61
62
63
64
65

1
2
3
4 106 depths. We also hypothesized that the community composition would differ more among depths
5
6 107 within sites than they would vary among sites separated by several kilometers if environmental
7
8 108 conditions vary across depths more than across sites. Differences in the relative abundance of
9
10 109 cryptic species across depths would allow ecologically similar species to co-exist at the reef scale
11
12 110 by increasing the potential effect of intraspecific competition on population size compared to
13
14 111 interspecific competition, or simply because of different responses among cryptic species to
15
16 112 environmental conditions.

20
21 113
22
23 114 **Materials and Methods**

24 115 *Description of the Pocillopora species complex.*

25
26 116 Corals in the genus *Pocillopora*, which dominate reefs throughout much of the Indo-
27
28 117 Pacific, contain separately evolving, genetically distinct lineages that are ‘hidden’ by
29
30 118 morphological similarity and plasticity. *Pocillopora* species can be delineated using the
31
32 119 mitochondrial open reading frame marker (mtORF, a gene which may play a role in the adaptive
33
34 120 response to environmental changes in pocilloporids (Banguera-Hinestrosa et al. 2019))
35
36 121 (Johnston et al. 2017), with the exception of *P. meandrina* and *P. eydouxi*, which can be
37
38 122 differentiated via a restriction fragment length polymorphism (RFLP) assay of the Histone 3
39
40 123 region (Johnston et al. 2018). The ability to use the mtORF marker and the RFLP assay to
41
42 124 delineate species is based on previous analyses comparing multiple genomic markers. In
43
44 125 previous phylogenetic analyses, Johnston et al. (2017) found strong concordance between
45
46 126 holobiont metagenomic data, transcriptomic data, near complete mitochondrial genomes, and
47
48 127 430 unlinked biallelic SNPs, and identified mtORF haplotype 1a - *P. eydouxi*, haplotype 1a - *P.*
49
50 128 *meandrina*, haplotype 2 (*P. cf. effusus*), haplotype 3b (belonging to *P. verrucosa*), haplotype 6a

1
2
3
4 129 (*P. ligulata*), haplotype 4 (*P. damicornis*), and haplotype 5 (*P. acuta*) as nominal species. The
5
6 130 strong concordance between these datasets and a time-calibrated phylogeny of mitochondrial
7
8 131 protein coding regions provide clear evidence of reciprocal monophyly with no evidence for
9
10 132 hybridization or incomplete lineage sorting for all but the two youngest sister species, *P.*
11
12 133 *damicornis* and *P. acuta* (which do not occur in our dataset) (Johnston et al. 2017). Using the
13
14 134 mtORF marker, Pinzón et al. (2013) identified haplotype 8a as a distinct lineage and Gélin et al.
15
16 135 (2017) identified mtORF haplotype 8a as a nominal species using two mitochondrial markers, a
17
18 136 nuclear marker, and 13 microsatellites. mtORF haplotype identification follows Pinzón et al.
19
20 137 (2013) and Forsman et al. (2013), and species names associated with each mtORF haplotype
21
22 138 follows Schmidt-Roach et al. (2014).
23
24 139
25
26 140 *Sampling design*
27
28
29
30
31 141 In August 2019, we sampled *Pocillopora* colonies from three depths (5, 10, and 20m) at
32
33 142 each of four sites (sites 1, 2, 4, and 5) on the fore reef of Mo'orea (Fig. 1). Site locations and
34
35 143 names correspond to that used by the Mo'orea Coral Reef Long-Term Ecological Research
36
37 144 (MCR-LTER) program (Holbrook et al. 2018). At each site, the sampling locations for each
38
39 145 depth were separated by horizontal distances in the order of 10's of meters. At each depth at each
40
41 146 site, 10-15 50 × 50 cm quadrats were randomly placed on the reef along the target depth contour
42
43 147 until approximately 50 colonies had been sampled. Tissue from all *Pocillopora* colonies within
44
45 148 the quadrat was sampled. Unlike previous studies, we did not target specific morphologies
46
47 149 (Edmunds et al 2016; De Palmas et al 2018). The number of *Pocillopora* colonies sampled at
48
49 150 each depth at each site ranged from 37 to 83 (Table 1). Tissue was collected from a total of 673
50
51 151 *Pocillopora* colonies. Tissue (~ 5 mm diameter) was collected using small bone clippers, stored
52
53
54
55
56
57
58
59
60
61
62
63
64
65

1
2
3
4 152 in salt-saturated dimethyl sulfoxide (DMSO) buffer (Gaither et al. 2011), and transported to
5
6 153 Florida State University for further processing.
7
8
9 154
10
11 155 *Genetic analysis and identification of genetic lineages*
12
13
14 156 Genomic DNA was extracted from tissues using Chelex 100 (Bio-Rad, USA). Samples
15
16 157 were incubated in 150 μ L of 10% Chelex 100 for 60 mins at 55°C followed by 15 mins at 95°C.
17
18
19 158 The supernatant was then used for PCR amplification using the mitochondrial Open Reading
20
21 159 Frame (mtORF) marker (Flot & Tillier, 2007). For the two species that cannot be differentiated
22
23 160 using this marker, *P. meandrina* and *P. eydouxi*, we used a restriction fragment length
24
25 polymorphism (RFLP) gel-based assay to distinguish the two following Johnston et al. (2018). In
26
27 161 GENEIOUS v.9.1.8 (Biomatters), forward mtORF sequences (855bp) were aligned and samples
28
29 162 were identified to haplotype based on previously published sequences of mtORF haplotypes,
30
31 163 using the naming conventions in Forsman et al. (2013) and Pinzón et al. (2013). We used the R
32
33 164 software package *pegas* (Paradis 2010) to construct the haplotype network.
34
35
36 165
37
38 166
39
40
41 167 *Environmental data*
42
43 168 We derived seven environmental variables related to sea water temperature and light
44
45 169 regimes at each site and depth (Fig. 1b – g):
46
47
48 170 1) the mean of the maximum daily sea water temperature from June to November ('Max Daily
49
50 171 Temp (Jun-Nov)'),
51
52
53 172 2) the mean of the maximum daily sea water temperature from December to May ('Max Daily
54
55 173 Temp (Dec-May)'),
56
57
58
59
60
61
62
63
64
65

1
2
3
4 174 3) the mean of the minimum daily sea water temperature from December to May ('Min Daily
5
6 175 Temp'),
7
8
9 176 4) the mean of the daily sea water temperature variance from December to May ('Temp Variance
10
11 177 [Mean']),
12
13
14 178 5) the maximum of the daily sea water temperature variance from December to May ('Temp
15
16 179 Variance [Max']),
17
18
19 180 6) the mean photosynthetically active radiation (PAR) from December to February ('Mean
20
21 181 Light'), and
22
23
24 182 7) the minimum PAR from December to February ('Min Light').
25

26 183 The sea water temperature regimes at 10 m and 20 m were quantified based on the *in situ*

27
28 184 time series (2005 – 2019) collected at 2 min intervals as part of the MCR-LTER program
29
30
31 185 (<http://mcrlter.msi.ucsb.edu/data/variable/>) using Seabird Electronics SBE39 and SBE56
32
33 186 temperature recorders (0.002 °C accuracy, 0.0001 °C resolution, < 10 s response time) mounted
34
35 187 onto plates directly affixed to the reef surface. Sea water temperatures for 5 m depth, where there
36
37 188 were no loggers, were derived for each site based on SST and the diurnal and semi-diurnal
38
39 189 variance observed at 2-min intervals in the backreef at 2 m and the fore reef at 10 m. Daily
40
41 190 average sea water temperatures at each depth was closely related to sea surface temperature
42
43
44 191 (SST), with SST explaining between 90-94%, 92-94%, 91-93%, 86-87%, and 78-80% of the
45
46
47 192 daily temperature variation at 2, 10, 20, 30 and 40 m, respectively. This allowed the derivation
48
49
50 193 of daily average sea water temperatures for 5 m depths at each site based on strong (r^2 of 0.988-
51
52
53 194 0.995) relationships describing changes in the SST-*in situ* relationships across depths. Daily
54
55 195 average sea water temperatures at 5 m were interpolated onto a 2-min grid and realistic
56
57
58 196 variability superimposed based on the time series of semi-diurnal and diurnal variability

1
2
3
4 197 observed at 2 m and 10 m at each site focusing on variations between 1 hr and the local inertial
5
6 198 period of 40 hrs (Wyatt et al. 2020).
7
8

9 199 PAR was derived for each site and depth based on satellite estimates of surface PAR
10
11 200 (Frouin et al. 2003) and the diffuse attenuation coefficient for PAR ($K_d(PAR)$); (Morel et al.
12
13 201 2007)) available from the European Space Agency GlobColour datasets over the period April
14
15 202 2016 to April 2020 (<http://www.globcolour.info/>). Daily PAR and $K_d(PAR)$ values were
16
17 203 obtained around Mo'orea at a $1/24^\circ$ resolution (approximately 6 x 6 km), with site specific
18
19 204 values based on the average of the nearest 4 pixels (approximately 12 x 12 km). Depth specific
20
21 205 PAR values (PAR_z) were then determined at 5, 10, and 20 m water depths at each site based on
22
23 206 the site-specific PAR and $K_d(PAR)$: $PAR_z(z) = PAR \cdot e^{-K_d(PAR) \cdot z}$.
24
25
26
27

28 207 A climatology was calculated for the time series of temperature and light at each site and
29
30 208 depth, which closely resembled bimodal normal distributions corresponding to summer and
31
32 209 winter seasons. Analyses focused on the summer-time temperature (December to May) and light
33
34 210 (December to February) regimes because we were specifically interested in how maximum daily
35
36 211 temperatures and the variance in temperature, which are both greatest in the summer months,
37
38 212 would serve as potential factors structuring *Pocillopora* communities. We also included the
39
40 213 mean of the maximum daily sea water temperature from June to November because it was the
41
42 214 main winter metric that differed among sites and depths in dissimilar ways to the summer
43
44 215 metrics.
45
46
47
48 216
49
50
51 217 *Statistical analyses*
52
53
54

55 218 Statistical analyses were performed in R v3.6.2 (R Core Team, 2019). We used binomial
56
57 219 generalized linear mixed models with base R function 'glm' to determine if *Pocillopora* relative
58
59
60
61
62
63
64
65

1
2
3
4 220 abundance differed by depth at each site. Distance-based Redundancy Analysis (db-RDA) was
5
6 221 used to analyze variation in the composition of *Pocillopora* haplotypes among depths and sites
7
8 222 (Legendre & Andersson, 1999; Legendre & Gallagher, 2001) using the *vegan* package in R
9
10 223 (Oksanen et al. 2019). db-RDA is a Redundancy Analysis (RDA) that analyzes the relationship
11
12 224 between principal coordinates, estimated using Bray-Curtis dissimilarity matrices on the raw
13
14 225 species data (proportion of samples from each species within each site and depth), and the
15
16 226 explanatory, or constraining, variables. In the first model, depth and site were the constraining
17
18 227 variables. In the second model, the seven environmental variables were the constraining
19
20 228 variables. The effects of the constraining variables were determined using a nonparametric
21
22 229 permutation test with 99999 permutations. Marginal tests of each factor indicate the unique
23
24 230 effect of each factor conditional on the presence of the other factor in the model. Ordination
25
26 231 biplots were used to visualize results and aid in interpretation.
27
28
29
30
31
32
33
34
35
36 232
37
38 233 **Results**
39
40
41 234 *Genetic identification*
42
43
44 235 Of the 673 *Pocillopora* samples, 14 mtORF haplotypes were identified, which include at
45
46 236 least six previously identified nominal species (Fig. 2). The majority of sampled colonies were
47
48 237 from two different species: *P. meandrina* (haplotype 1a, n = 273) and haplotype 10 (n = 187). At
49
50 238 Mo'orea, *P. meandrina* is often visibly indistinguishable from *P. verrucosa* and haplotype 10 in
51
52 239 the field based on gross morphology but differs by at least 20 (2%) mtORF base pairs (Fig. 2).
53
54 240 Haplotype 10 is most genetically similar to haplotypes previously described as *P. verrucosa* (3a,
55
56 241 n = 7; 3b, n = 22; 3f, n = 3, and 3h, n = 2) (Schmidt-Roach et al. 2014), but still differs by 5 – 8
57
58 242 bp. Haplotype 10 has only been documented at Mo'orea and surrounding islands (Forsman et al.
59
60
61
62
63
64
65

1
2
3
4 243 2013; Mayfield et al. 2015; Edmunds et al. 2016; Gélin et al. 2017). Haplotype 8a (n = 72) is
5
6 244 most genetically similar to *P. meandrina* and *P. eydouxi* (haplotype 1a, n = 53), differing by 7
7
8 245 bp. Haplotype 2 (n = 6) and haplotype 11 (n = 38) differ by 4 bp. Haplotype 11 is also closely
9
10 246 related to haplotype 6a (*P. ligulata*), differing by only two base pair substitutions (mtORF
11
12 247 sequences 99.8% identical over 855bp; Fig. 2), but is morphologically most similar to *P.*
13
14 248 *eydouxi*. Haplotype 9 (n = 3), previously documented from Mo'orea (Forsman et al. 2013),
15
16 249 differs by 1 bp from *P. meandrina* and *P. eydouxi* (haplotype 1a). All but four haplotypes have
17
18 250 been documented from previous mtORF analyses of *Pocillopora*. They include three haplotypes
19
20 251 that each differed from *P. meandrina* and *P. eydouxi* (haplotype 1a) by one bp (haplotype 1c, n =
21
22 252 3; haplotype 1d, n = 1; haplotype 1e, n = 2), and one haplotype that differed from haplotype 11
23
24 253 by one bp (n = 1).
25
26
27
28
29
30
31 254
32
33 255 *Depth distribution*
34
35
36 256 The relative abundance of the most abundant species (*P. meandrina*, haplotype 10, and
37
38 257 haplotype 8a) differed among depths (Fig. 3). For example, at 5m depth, 49% to 73% of
39
40 258 *Pocillopora* colonies were *P. meandrina*, and only 0% to 5% were haplotype 10, depending on
41
42 259 the site. At 20m depth, only 0% to 21% of *Pocillopora* colonies were *P. meandrina*, whereas
43
44 260 44% to 81% of colonies were haplotype 10. At site 4, the relative abundance of *P. meandrina* did
45
46 261 not differ between 5 and 10 m, but the species was not present in our sampling at 20 m. Site 4
47
48 262 was also the only site at which haplotype 11 was sampled at all depths. For the less abundant
49
50 263 species (haplotype 11, *P. eydouxi*, and *P. verrucosa* haplotype 3b), there were little to no
51
52 264 differences in their relative abundances across depths (Fig. 3). *P. eydouxi* was relatively rare but
53
54 265 was the only species in our collection that was sampled from all sites and depths.
55
56
57
58
59
60
61
62
63
64
65

1
2
3
4 266
5
6
7 267 *Community composition*
8
9 268 The composition of *Pocillopora* haplotypes varied across depths, but not among sites
10
11 269 (Table 2, Fig. 4a). In the analysis using depth and site as the constraining variables, the first
12
13 270 dbRDA axis explained 79.72% of the variation in community dissimilarity and was most
14
15 271 associated with differences across depths. The *Pocillopora* community at 5 m was characterized
16
17 272 by relatively high abundance of *P. meandrina*. The *Pocillopora* community at 20 m was
18
19 273 characterized by relatively high abundance of haplotype 10. The second dbRDA axis explained
20
21 274 6.67% of the variation in community dissimilarity and was associated with differences across
22
23 275 sites. In the analysis constrained using the environmental variables (Fig. 4b), the *Pocillopora*
24
25 276 community at 20 m was associated with higher daily temperature variance, lower minimum daily
26
27 277 temperatures in December – May, and lower maximum daily temperatures in June - November.
28
29 278 Maximum daily temperature in December – May, on the other hand, was more associated with
30
31 279 community differences between the north shore (Site 1 and 2, higher maximum daily
32
33 280 temperature) vs the southern shore (Site 4 and 5, lower maximum daily temperature) than it was
34
35 281 between depths. The *Pocillopora* community at 5 m was associated with higher mean and
36
37 282 minimum daily light.
38
39 283
40
41 284 **Discussion**
42
43
44 285 Cryptic species, because of their morphological similarity, are often considered to be
45
46 286 ecologically similar, so would not be expected to exhibit stable coexistence if competing for the
47
48 287 same limiting resource. However, empirical explanations for why exactly cryptic species
49
50 288 commonly co-occur in a particular circumstance remain elusive (Zhang et al. 2004; McPeek and
51
52
53
54
55
56
57
58
59
60
61
62
63
64
65

1
2
3
4 289 Gomulkiewicz 2005; De Meester et al. 2011; Montero-Pau et al. 2011). From extensive sampling
5 around the island of Mo'orea and at multiple depths, we genetically identified 673 colonies in the
6
7 290 *Pocillopora* species complex, without limiting sampling towards certain morphological
8 characters, and uncovered differences among haplotypes in their relative abundance at each
9
10 291 depth. Most of the dominant haplotypes are known to be evolutionarily distinct genetic lineages,
11 or genetic species (Gélin et al. 2017; Johnston et al. 2017; Schmidt-Roach et al. 2014). We found
12
13 292 that differences in species composition across depths within a site across 10's of meters were
14
15 293 greater than differences among sites separated by several kilometers. Consistent with internal-
16
17 294 wave cooling found at Mo'orea (Wyatt et al. 2020), we also show that the temporal variance in
18
19 295 sea water temperatures increased with depth and were more associated with the *Pocillopora*
20
21 296 community composition at 20 m than were maximum daily temperatures.
22
23
24 297
25
26 298
27
28 299
29
30
31 300 Species must co-occur to directly interact, but the degree of co-occurrence does not
32
33 301 necessarily reflect the degree to which species interact (Blanchet et al. 2020). Therefore, while
34
35 302 we have identified differences among cryptic species in their relative abundance across a depth
36
37 303 gradient, and associations with environmental variables that co-vary with depth, we cannot yet
38
39 304 determine whether such ecological differences are driven by species interactions (e.g.,
40
41 305 competition) or difference in the response of species to abiotic environmental conditions, or
42
43 306 both. For example, the observed depth patterns could be influenced by larval habitat selection
44
45 307 and post-settlement mortality, both of which could be determined by the presence of other
46
47 308 species as well as the abiotic environment (Mundy and Babcock 1998, Baird et al. 2003, Hunt
48
49 309 and Scheibling 1997, Penin et al. 2010). Furthermore, the depth segregation of species could be
50
51 309
52
53 310 facilitated by dispersal limitation of negatively buoyant eggs in benthic boundary layers (Hirose
54
55 310
56
57 311 et al. 2000; Schmidt-Roach et al. 2012), and the relatively fast development of larval motility
58
59
60
61
62
63
64
65

1
2
3
4 312 (only 8 hrs in *P. eydouxi* (Hirose et al. 2000) compared with up to 96 hrs in acroporid corals
5
6 313 (Miller and Ball 2000)).
7
8

9 314 Divergent selection between adjacent habitats can both form new species and maintain
10
11 315 closely related species, despite the lack of physical barriers preventing the dispersal of marine
12
13 316 larvae among habitats (Rocha et al. 2005; González et al. 2018; Whitney et al. 2018). Changes in
14
15 317 environmental conditions associated with depth gradients have been hypothesized to serve as
16
17 318 axes of speciation in corals (Carlon and Budd 2002; Bongaerts et al. 2010, 2013, 2021; Levitan
18
19 319 et al. 2011; Prada and Hellberg 2013, 2021). At Mo’orea, the four most abundant *Pocillopora*
20
21 320 species, which are often visibly indistinguishable at the gross colony level, exhibited stark
22
23 321 differences in their relative abundance across depths – *P. meandrina* and haplotype 8a were often
24
25 322 more abundant at 5 m than at 10 m and 20 m, while haplotype 10 and *P. verrucosa* haplotype 3b
26
27 323 were more abundant at 20 m than at 10 and 5 m (Fig. 3). In Taiwan, De Palmas et al. (2018)
28
29 324 targeted sampling of the “*P. verrucosa* morphotype,” and also found that samples genetically
30
31 325 identified as *P. verrucosa* (haplotypes 3a, 3b, 3f, 3g, 3h) were more prevalent on deeper reefs (23
32
33 326 – 45 m), while *P. meandrina* and haplotype 8a were more prevalent on shallow reefs (7 – 15 m).
34
35 327 Haplotype 10 is most closely related to *P. verrucosa* haplotype 3b (Fig. 2) yet, although more
36
37 328 dominant, shares the same depth distribution, which would be inconsistent with an expectation of
38
39 329 speciation by depth. However, *P. verrucosa* haplotype 3b has a widespread distribution
40
41 330 (documented from the Galapagos to the Red Sea (Pinzón et al., 2013; Sawall et al., 2015)), while
42
43 331 haplotype 10 has only been documented from French Polynesia (Forsman et al. 2013; Mayfield
44
45 332 et al. 2015; Gélin et al. 2017). The apparent endemicity of haplotype 10 to French Polynesia is
46
47 333 consistent with the hypothesis that this haplotype diverged from *P. verrucosa* in this region, but
48
49
50
51
52
53
54
55
56
57
58
59
60
61
62
63
64
65

1
2
3
4 334 because these lineages share similar niche space with respect to depth, the conditions that led to
5
6
7 335 their divergence require further investigation.
8

9 336 The sampling of clones was unlikely in our study. Brooding *Pocillopora* species (e.g., *P.*
10
11 337 *damicornis* and *P. acuta*) are known to produce asexual larvae (Combosch and Vollmer 2013;
12
13 338 Torda et al. 2013), but we did not observe any of the brooding *Pocillopora* species on the fore
14
15 339 reef of Mo’orea. Clonal stands of broadcast spawning *Pocillopora* species have been observed in
16
17 340 the Gulf of California and in the Galapagos as a result of branch fragmentation and reattachment,
18
19 341 and not the release of clonal larvae (Pinzón et al. 2012; Baums et al., 2014). However, we did not
20
21 342 find visible evidence for branch reattachment to the reef via fragmentation at any of our sites. In
22
23 343 contrast to the large monospecific stands that form in the Tropical Eastern Pacific, individual
24
25 344 *Pocillopora* colonies are distinct and can be easily distinguished on the fore reef of Mo’orea,
26
27 345 which is aided by the fact that colonies are all less than ~10 years old (Adam et al. 2011).
28
29 346 Furthermore, Magalon, Adjeroud, & Veuille (2005) found no genetic evidence of clones when
30
31 347 sampling colonies displaying the “*P. meandrina* morphology” on Mo’orea and throughout
32
33 348 French Polynesia.
34
35 349 Differences in the relative abundance of species across a fairly narrow depth range (5 –
36
37 350 20 m) indicates that there are biological differences among cryptic species. Therefore, these
38
39 351 cryptic species are not ecologically similar (see also Burgess et al. (2021)) and should not be
40
41 352 grouped and analyzed as a single group, as is commonly done (Darling et al. 2013; Pratchett et
42
43 353 al. 2013; Tsounis and Edmunds 2016). Our results indicate that *P. meandrina* and haplotype 8a
44
45 354 are genetically and ecologically divergent from haplotype 10 and *P. verrucosa* haplotype 3b, yet
46
47 355 these four haplotypes cannot be reliably identified in the field based on morphology (Fig. 3).
48
49 356 Additionally, *P. eydouxi* is morphologically indistinguishable from haplotype 11, but exhibited a
50
51
52
53
54
55
56
57
58
59
60
61
62
63
64
65

1
2
3
4 357 different depth distribution pattern. All six of these haplotypes are morphologically
5
6 358 indistinguishable when small (<approx. 25 cm diameter). To properly capture biodiversity
7
8 359 patterns, sampling needs to be stratified by depth, not just occur horizontally across different
9
10 360 locations, and should not rely on morphological characters to identify genetically and
11
12 361 ecologically different species.
13
14
15

16 362 Depth differences in the community composition of *Pocillopora* were associated with
17
18 363 temperature and light regimes. *P. meandrina* and haplotype 8a dominated shallower locations
19
20 364 with higher light irradiance, higher daily temperature minimums, and lower temperature variance
21
22 365 (Fig. 4). Haplotype 10 and *P. verrucosa* haplotype 3b dominated deeper locations with lower
23
24 366 irradiance, lower daily temperature minimums, and higher temperature variance. The increased
25
26 367 temperature variance, and lower daily temperature minimums, with depth is a signature of the
27
28 368 internal wave climate and the increased extent to which internal waves bring cooler water to
29
30 369 deeper sections of the reef slope (Wyatt et al. 2020). Depth distributions of *P. meandrina*,
31
32 369
33 370 haplotype 8a, haplotype 10, and *P. verrucosa* haplotype 3b therefore seem more sensitive to
34
35 370 frequent cooling in deeper water than to periodic heating more likely in shallower water due to
36
37 371 increased solar irradiance. The current distribution of haplotype 11, however, does appear to
38
39 372 reflect the impacts of more prolonged heating. In 2019, a prolonged ocean heating event (several
40
41 373 weeks) caused widespread coral bleaching in *Pocillopora* at Mo'orea, with subsequent mortality
42
43 374 much higher for haplotype 11 than any of the other *Pocillopora* species (Burgess et al. 2021).
44
45
46 375 Heat accumulation and bleaching mortality was also greatest at site 1 and 2, intermediate at site
47
48 376 5, and the least at site 4, which might explain the differences in the *Pocillopora* community
49
50 377 among sites seen in Fig 4. These data suggest that the niche space of haplotype 11 is more
51
52 378 constrained by heat stress than that of the other cooccurring species. The lack of differentiation
53
54
55 379
56
57
58
59
60
61
62
63
64
65

1
2
3
4 380 in abundance by depth or site observed for *P. eydouxi* indicates that this species has a broader
5
6
7 381 niche space with respect to depth than other co-occurring *Pocillopora* species.
8
9 382 Any differences in the *Symbiodiniaceae* community hosted by each *Pocillopora*
10
11 383 haplotype could also be associated with their depth specificity. *Pocillopora* species typically host
12
13 384 *Symbiodiniaceae* from a single genus, but under certain conditions are capable of shuffling their
14
15 385 symbiont communities in response to environmental changes (McGinley et al. 2012; Rouzé et al.
16
17 386 2019). Both brooding and broadcast spawning *Pocillopora* vertically transmit their
18
19 387 photosynthetic symbionts (Glynn et al. 1991; Schmidt-Roach et al. 2012; Massé et al. 2013;
20
21 388 Johnston et al. 2020), and there is some evidence that *Symbiodiniaceae* associations differ
22
23 389 between *Pocillopora* species (Cunning et al. 2013; Brener-Raffalli et al. 2018).
24
25
26
27
28 390 Finally, the identification of differences among cryptic species in their relative abundance
29
30 391 across depths has important implications for response diversity (*sensu* Emlqvist et al. 2003).
31
32
33 392 Response diversity can maintain ecosystem states when species sharing similar ecological
34
35 393 functions, afforded by their similar morphology, differ in their response to perturbations, such
36
37 394 that the temporary loss of one species is compensated by less impacted species (Chapin et al.
38
39 395 1997; Yachi and Loreau 1999). We have previously shown differences among cryptic
40
41 396 *Pocillopora* species at Mo'orea in their response to a recent bleaching event (Burgess et al.
42
43 397 2021). However, response diversity enhances resilience only when there are niche differences
44
45 398 and spatial variation in the relative abundance among species (Baskett et al. 2014). Our results
46
47 399 here, therefore, strengthen the case for response diversity as an explanation for the seemingly
50
51 400 unusual patterns of recovery in *Pocillopora* known for Mo'orea (Kayal et al. 2018; Edmunds et
52
53 401 al. 2019).
54
55
56
57
58 402

1
2
3
4 403 On behalf of all authors, the corresponding author states that there is no conflict of interest.
5
6
7 404
8
9 405 **Acknowledgements:**
10
11 406 This work was funded by a National Science Foundation (NSF) grant to S. C. Burgess (OCE 18-
12
13
14 407 29867). We thank J. Powell and C. Peters for invaluable assistance in the field, C. Peters and the
15
16 408 Florida State University Dive Program for facilitating field work on SCUBA, the staff of the UC
17
18
19 409 Berkeley Richard B. Gump South Pacific Research Station for facilitating our research, and M.
20
21 410 Hay for logistical support. Research was completed under permits issued by the French
22
23
24 411 Polynesian Government (Délégation à la Recherche), the Haut-Commissariat de la République
25
26 412 en Polynésie Française (DTRT) (Protocole d'Accueil 2019), and the U.S. Fish and Wildlife. A.
27
28
29 413 S. J. Wyatt was supported by funding from the Hong Kong Branch of the Southern Marine
30
31 414 Science and Engineering Guangdong Laboratory (Guangzhou) (SMSEGL20SC01) and the
32
33 415 Research Grants Council (RGC) of Hong Kong (RGC Project No. 26100120).
34
35
36 416
37
38 417 **Data Accessibility:**
39
40
41 418 R scripts and data used to perform analyses and prepare figures are available at Dryad (link
42
43 419 provided upon acceptance).
44
45
46 420
47
48 421 **Literature cited**
49
50
51 422 Adam TC, Schmitt RJ, Holbrook SJ, Brooks AJ, Edmunds PJ, Carpenter RC, Bernardi G (2011)
52 423 Herbivory, connectivity, and ecosystem resilience: Response of a coral reef to a large-scale
53 424 perturbation. PLoS One 6:e23717
54 425 Baird AH, Babcock RC, Mundy CP (2003) Habitat selection by larvae influences the depth
55 426 distribution of six common coral species. Mar Ecol Prog Ser 252:289–293
56
57 427 Banguera-Hinestrosa E, Ferrada E, Sawall Y, Flot JF (2019) Computational characterization of
58 428 the mtORF of Pocilloporid Corals: Insights into protein structure and function in *Stylophora*
59 429 lineages from contrasting Environments. Genes 10(324):1-30
60
61
62
63
64
65

1
2
3
4 430 Baskett ML, Fabina NS, Gross K (2014) Response diversity can increase ecological resilience to
5 431 disturbance in coral reefs. *Am Nat* 184:E16–E31
6
7 432 Baums IB, Devlin-Durante M, Laing BAA, Feingold J, Smith T, Bruckner A, Monteiro J (2014)
8 433 Marginal coral populations: the densest known aggregation of *Pocillopora* in the Galapagos
9 434 Archipelago is of asexual origin. *Front Mar Sci* 1:1–11
10 435 Berkley HA, Kendall BE, Mitarai S, Siegel DA (2010) Turbulent dispersal promotes species
11 436 coexistence. *Ecol Lett* 13:360–371
12
13 437 Bickford D, Lohman DJ, Sodhi NS, Ng PKL, Meier R, Winker K, Ingram KK, Das I (2007)
14 438 Cryptic species as a window on diversity and conservation. *Trends Ecol Evol* 22:148–155
15 439 Blanchet FG, Cazelles K, Gravel D (2020) Co-occurrence is not evidence of ecological
16 440 interactions. *Ecol Lett* 23:1050–1063
17
18 441 Bode M, Bode L, Armsworth PR (2011) Different dispersal abilities allow reef fish to coexist.
19 442 *Proc Natl Acad Sci U S A* 108:16317–16321
20 443 Bongaerts P, Cooke IR, Ying H, Wels D, Haan den S, Hernandez-Agreda A, Brunner CA, Dove
21 444 S, Englebert N, Eyal G, Forêt S, Grinblat M, Hay KB, Harii S, Hayward DC, Lin Y,
22 445 Mihaljević M, Moya A, Muir P, Sinniger F, Smallhorn-West P, Torda G, Ragan MA, van
23 446 Oppen MJH, Hoegh-Guldberg O (2021) Morphological stasis masks ecologically divergent
24 447 coral species on tropical reefs. *Curr Biol* 1–13
25
26 448 Bongaerts P, Frade PR, Ogier JJ, Hay KB, Van Bleijswijk J, Englebert N, Vermeij MJ, Bak RP,
27 449 Visser PM, Hoegh-Guldberg O (2013) Sharing the slope: Depth partitioning of Agariciid
28 450 corals and associated *Symbiodinium* across shallow and mesophotic habitats (2–60 m) on a
29 451 Caribbean reef. *BMC Evol Biol* 13:205
30
31 452 Bongaerts P, Riginos C, Ridgway T, Sampayo EM, van Oppen MJH, Englebert N, Vermeulen F,
32 453 Hoegh-Guldberg O (2010) Genetic divergence across habitats in the widespread coral
33 454 *Seriatopora hystrix* and its associated *Symbiodinium*. *PLoS One* 5:e10871
34
35 455 Boulay JN, Hellberg ME, Cortés J, Baums IB (2014) Unrecognized coral species diversity masks
36 456 differences in functional ecology. *Proc Biol Sci* 281:20131580
37
38 457 Bouwmeester J, Berumen ML, Baird AH (2011) Daytime broadcast spawning of *Pocillopora*
39 458 *verrucosa* on coral reefs of the central Red Sea. *Galaxea, J Coral Reef Stud* 13:23–24
40
41 459 Brener-Raffalli K, Clerissi C, Vidal-Dupiol J, Adjeroud M, Bonhomme F, Pratlong M, Aurelle
42 460 D, Mitta G, Toulza E (2018) Thermal regime and host clade, rather than geography, drive
43 461 *Symbiodinium* and bacterial assemblages in the scleractinian coral *Pocillopora damicornis*
44 462 sensu lato. *Microbiome* 6(39):1–13
45
46 463 Burgess SC, Johnston EC, Wyatt ASJ, Leichter JJ, Edmunds PJ (2021) Response diversity in
47 464 corals: hidden differences in bleaching mortality among cryptic *Pocillopora species*.
48 465 *Ecology*: e03324
49
50 466 Carlon DB, Budd AF (2002) Incipient speciation across a depth gradient in a scleractinian coral?
51 467 *Evolution* 56:2227–42
52
53 468 Chapin FS, Walker BH, Hobbs RJ, Hooper DU, Lawton JH, Sala OE, Tilman D (1997) Biotic
54 469 control over the functioning of ecosystems. *Science* 277:500–504
55
56 470 Chesson P (2000) Mechanisms of maintenance of species diversity. *Annu Rev Ecol Syst* 31:343–
57 471 366
58
59 472 Combosch DJ, Vollmer S V. (2013) Mixed asexual and sexual reproduction in the Indo-Pacific
60 473 reef coral *Pocillopora damicornis*. *Ecol Evol* 1–9
61
62 474 Cunning R, Glynn PW, Baker AC (2013) Flexible associations between *Pocillopora* corals and
63 475 *Symbiodinium* limit utility of symbiosis ecology in defining species. *Coral Reefs* 32:795–

1
2
3
4 476 801
5 477 Daly AJ, De Meester N, Baetens JM, Moens T, De Baets B (2021) Untangling the mechanisms
6 478 of cryptic species coexistence in a nematode community through individual- based
7 479 modelling. *Oikos* 130: 587-600
8 480 Darling ES, McClanahan TR, Côté IM (2013) Life histories predict coral community
9 481 disassembly under multiple stressors. *Glob Chang Biol* 19:1930–40
10 482 Edmunds P, Adam T, Baker A, Doo S, Glynn P, Manzello D, Silbiger N, Smith T, Fong P (2019)
11 483 Why more comparative approaches are required in time-series analyses of coral reef
12 484 ecosystems. *Mar Ecol Prog Ser* 608:297–306
13 485 Edmunds PJ, Leichter JJ, Johnston EC, Tong EJ, Toonen RJ (2016) Ecological and genetic
14 486 variation in reef-building corals on four Society Islands. *Limnol Oceanogr* 61:543–557
15 487 Elmquist T, Folke C, Nyström M, Peterson G, Bengtsson J, Walker B, Norberg J (2003)
16 488 Response diversity, ecosystem change, and resilience. *Front Ecol Environ* 1:488–494
17 489 Flot JF, Magalon H, Cruaud C, Couloux A, Tillier S (2008) Patterns of genetic structure among
18 490 Hawaiian corals of the genus *Pocillopora* yield clusters of individuals that are compatible
19 491 with morphology. *Comptes Rendus - Biol* 331:239–247
20 492 Flot JF, Tillier S (2007) The mitochondrial genome of *Pocillopora* (Cnidaria: Scleractinia)
21 493 contains two variable regions: The putative D-loop and a novel ORF of unknown function.
22 494 *Gene* 401:80–87
23 495 Forsman ZH, Johnston EC, Brooks AJ, Adam TC, Toonen RJ (2013) Genetic evidence for
24 496 regional isolation of *Pocillopora* corals from Moorea. *Oceanography* 26:153–155
25 497 Frouin R, Franz BA, Werdell PJTSP product. (2003) The SeaWiFS PAR product. In: Hooker
26 498 S.B., Firestone E.R. (eds) Algorithm Updates for the Fourth SeaWiFS Data Reprocessing:
27 499 NASA Technical Memo 2003-206892. NASA Goddard Space Flight Center, Greenbelt,
28 500 Maryland, pp 46–50
29 501 Gaither MR, Szabó Z, Crepeau MW, Bird CE, Toonen RJ (2011) Preservation of corals in salt-
30 502 saturated DMSO buffer is superior to ethanol for PCR experiments. *Coral Reefs* 30:329–
31 503 333
32 504 Gélin P, Postaire B, Fauvelot C, Magalon H (2017) Reevaluating species number, distribution
33 505 and endemism of the coral genus *Pocillopora* Lamarck, 1816 using species delimitation
34 506 methods and microsatellites. *Mol Phylogenet Evol* 109:430–446
35 507 Glynn PW, Gassman NJ, Eakin CM, Cortes J, Smith DB, Guzman HM (1991) Reef coral
36 508 reproduction in the eastern Pacific: Costa Rica, Panama and Galápagos Islands (Ecuador).
37 509 Part I. *Pocilloporidae*. *Mar Biol* 109:355–368
38 510 Gómez- Corrales M, Prada C (2020) Cryptic lineages respond differently to coral bleaching.
39 511 *Mol Ecol* 29:4265–4274
40 512 González AM, Prada CA, Ávila V, Medina M (2018) Ecological speciation in corals. In:
41 513 Oleksiak M., Rajora O. (eds) Population genomics: Marine organisms. Population
42 514 genomics. Springer, Cham.
43 515 Hirose M, Kinzie RA, Hidaka M (2000) Early development of zooxanthella-containing eggs of
44 516 the corals *Pocillopora verrucosa* and *P. eydouxi* with special reference to the distribution of
45 517 zooxanthellae. *Biol Bull* 199:68–75
46 518 Holbrook SJ, Adam TC, Edmunds PJ, Schmitt RJ, Carpenter RC, Brooks AJ, Lenihan HS,
47 519 Briggs CJ (2018) Recruitment drives spatial variation in recovery rates of resilient coral
48 520 reefs. *Sci Rep* 8:7338
49 521 Hunt HL, Scheibling RE (1997) Role of early post-settlement mortality in recruitment of benthic
50
51
52
53
54
55
56
57
58
59
60
61
62
63
64
65

1
2
3
4 522 marine invertebrates. *Mar Ecol Prog Ser* 155:269–301
5 523 Johnston EC, Counsell CW, Sale TL, Burgess SC, Toonen RJ (2020) The legacy of stress: Coral
6 524 bleaching impacts reproduction years later. *Funct Ecol* 34:2315–2325
7 525 Johnston EC, Forsman ZH, Flot J, Schmidt-Roach S, Pinzón J, Knapp ISS, Toonen RJ (2017) A
8 526 genomic glance through the fog of plasticity and diversification in *Pocillopora*. *Sci Rep*
9 527 7:5991
10 528 Johnston EC, Forsman ZH, Toonen RJ (2018) A simple molecular technique for distinguishing
11 529 species reveals frequent misidentification of Hawaiian corals in the genus *Pocillopora*.
12 530 PeerJ 6: e4355
13 531 Kayal M, Lenihan HS, Brooks AJ, Holbrook SJ, Schmitt RJ, Kendall BE (2018) Predicting coral
14 532 community recovery using multi-species population dynamics models. *Ecol Lett* 22:605–
15 533 615
16 534 Knowlton N, Weil E, Weigt LA, Guzmán HM (1992) Sibling species in *Montastraea annularis*,
17 535 coral bleaching, and the coral climate record. *Science* 255:330–333
18 536 Legendre P, Andersson MJ (1999) Distance-based redundancy analysis: Testing multispecies
19 537 responses in multifactorial ecological experiments. *Ecol Monogr* 69:1–24
20 538 Legendre P, Gallagher ED (2001) Ecologically meaningful transformations for ordination of
21 539 species data. *Oecologia* 129:271–280
22 540 Levin SA, Lubchenco J (2008) Resilience, robustness, and marine ecosystem-based
23 541 management. *Bioscience* 58:27–32
24 542 Levitán DR (2004) Density-dependent sexual selection in external fertilizers: Variances in male
25 543 and female fertilization success along the continuum from sperm limitation to sexual
26 544 conflict in the sea urchin *Strongylocentrotus franciscanus*. *Am Nat* 164:298–309
27 545 Levitán DR, Fogarty ND, Jara J, Lotterhos KE, Knowlton N (2011) Genetic, spatial, and
28 546 temporal components of precise spawning synchrony in reef building corals of the
29 547 *Montastraea annularis* species complex. *Evolution* 65:1254–70
30 548 Magalon H, Adjeroud M, Veuille M (2005) Patterns of genetic variation do not correlate with
31 549 geographical distance in the reef-building coral *Pocillopora meandrina* in the South Pacific.
32 550 *Mol Ecol* 14:1861–1868
33 551 Marti-Puig P, Forsman ZH, Haverkort-yeh RD, Knapp ISS, Maragos JE, Toonen RJ (2014)
34 552 Extreme phenotypic polymorphism in the coral genus *Pocillopora*; micro-morphology
35 553 corresponds to mitochondrial groups, while colony morphology does not. *Bull Mar Sci*
36 554 90:1–22
37 555 Massé LM, Séré MG, Smit AJ, Schleyer MH (2013) Sexual reproduction in *Pocillopora*
38 556 *damicornis* at high latitude off South Africa. *West Indian Ocean J Mar Sci* 11:55–65
39 557 Mayfield AB, Bruckner AW, Chen C, Chen C (2015) A survey of pocilloporid corals and their
40 558 endosymbiotic dinoflagellate communities in the Austral and Cook Islands of the South
41 559 Pacific. *Platax* 12:1–17
42 560 Mayfield MM, Levine JM (2010) Opposing effects of competitive exclusion on the phylogenetic
43 561 structure of communities. *Ecol Lett* 13:1085–1093
44 562 McGinley MP, Aschaffenburg MD, Pettay DT, Smith RT, LaJeunesse TC, Warner ME (2012)
45 563 *Symbiodinium* spp. in colonies of eastern Pacific *Pocillopora* spp. are highly stable despite
46 564 the prevalence of low-abundance background populations. *Mar Ecol Prog Ser* 462:1–7
47 565 McPeek MA, Gomulkiewicz R (2005) Assembling and depleting species richness in
48 566 metacommunities: Insights from ecology, population genetics and macroevolution. In: M.
49 567 Holyoak et al. (eds) *Metacommunities: Spatial Dynamics and Ecological Communities*.
50
51
52
53
54
55
56
57
58
59
60
61
62
63
64
65

1
2
3
4 568 Chicago (IL): University of Chicago, pp 355–373
5 569 De Meester N, Derycke S, Bonte D, Moens T (2011) Salinity effects on the coexistence of
6 570 cryptic species: A case study on marine nematodes. *Mar Biol* 158:2717–2726
7 571 Miller DJ, Ball EE (2000) The coral *Acropora*: What it can contribute to our knowledge of
8 572 metazoan evolution and the evolution of developmental processes. *BioEssays* 22:291–296
9 573 Montero-Pau J, Ramos-Rodríguez E, Serra M, Gómez A (2011) Long-term coexistence of rotifer
10 574 cryptic species. *PLoS One* 6:e21530
11 575 Morel A, Huot Y, Gentili B, Werdell PJ, Hooker SB, Franz BA (2007) Examining the
12 576 consistency of products derived from various ocean color sensors in open ocean (Case 1)
13 577 waters in the perspective of a multi-sensor approach. *Remote Sens Environ* 111:69–88
14 578 Mundy CN, Babcock RC (1998) Role of light intensity and spectral quality in coral settlement:
15 579 Implications for depth-dependent settlement? *J Exp Mar Bio Ecol* 223:235–255
16 580 Oksanen J, Blanchet F, Friendly M, Kindt R, Legendre P, McGlinn D, Minchin P, O'Hara R,
17 581 Simpson G, Solymos P, Stevens M, Szoecs E, Wagner H (2019) Vegan: Community
18 582 Ecology Package. R package version 2.5-6.
19 583 <https://cran.r-project.org/web/packages/vegan/index.html>
20 584 De Palmas S, Soto D, Denis V, Ho M-J, Chen CA (2018) Molecular assessment of *Pocillopora*
21 585 *verrucosa* (Scleractinia; Pocilloporidae) distribution along a depth gradient in Ludao,
22 586 Taiwan. *PeerJ* 6:e5797
23 587 Paradis E (2010) Pegas: An R package for population genetics with an integrated-modular
24 588 approach. *Bioinformatics* 26:419–420
25 589 Paz-García DA, Hellberg ME, García-de-León FJ, Balart EF (2015a) Switch between
26 590 morphospecies of *Pocillopora* corals. *Am Nat* 186:434–440
27 591 Paz-García DA, Aldana-Moreno A, Cabral-Tena RA, García-De-León FJ, Hellberg ME, Balart
28 592 EF (2015b) Morphological variation and different branch modularity across contrasting
29 593 flow conditions in dominant *Pocillopora* reef-building corals. *Oecologia* 178:207–218
30 594 Penin L, Michonneau F, Baird A, Connolly S, Pratchett M, Kayal M, Adjeroud M (2010) Early
31 595 post-settlement mortality and the structure of coral assemblages. *Mar Ecol Prog Ser*
32 596 408:55–64
33 597 Pinzon JH, LaJeunesse TC (2011) Species delimitation of common reef corals in the genus
34 598 *Pocillopora* using nucleotide sequence phylogenies, population genetics and symbiosis
35 599 ecology. *Mol Ecol* 20:311–325
36 600 Pinzón JH, Reyes-Bonilla H, Baums IB, LaJeunesse TC (2012) Contrasting clonal structure
37 601 among *Pocillopora* (Scleractinia) communities at two environmentally distinct sites in the
38 602 Gulf of California. *Coral Reefs* 31:765–777
39 603 Pinzón JH, Sampayo E, Cox E, Chauka LJ, Chen CA, Voolstra CR, LaJeunesse TC (2013) Blind
40 604 to morphology: genetics identifies several widespread ecologically common species and
41 605 few endemics among Indo-Pacific cauliflower corals (*Pocillopora*, Scleractinia). *J Biogeogr*
42 606 40:1595–1608
43 607 Prada C, Hellberg ME (2013) Long prereproductive selection and divergence by depth in a
44 608 Caribbean candelabrum coral. *Proc Natl Acad Sci U S A* 110:3961–6
45 609 Prada C, Hellberg ME (2021) Speciation-by-depth on coral reefs: Sympatric divergence with
46 610 gene flow or cryptic transient isolation? *J Evol Biol* 34:128–137
47 611 Pratchett MS, McCowan D, Maynard JA, Heron SF (2013) Changes in bleaching susceptibility
48 612 among corals subject to ocean warming and recurrent bleaching in Moorea, French
49 613 Polynesia. *PLoS One* 8:e70443
50
51
52
53
54
55
56
57
58
59
60
61
62
63
64
65

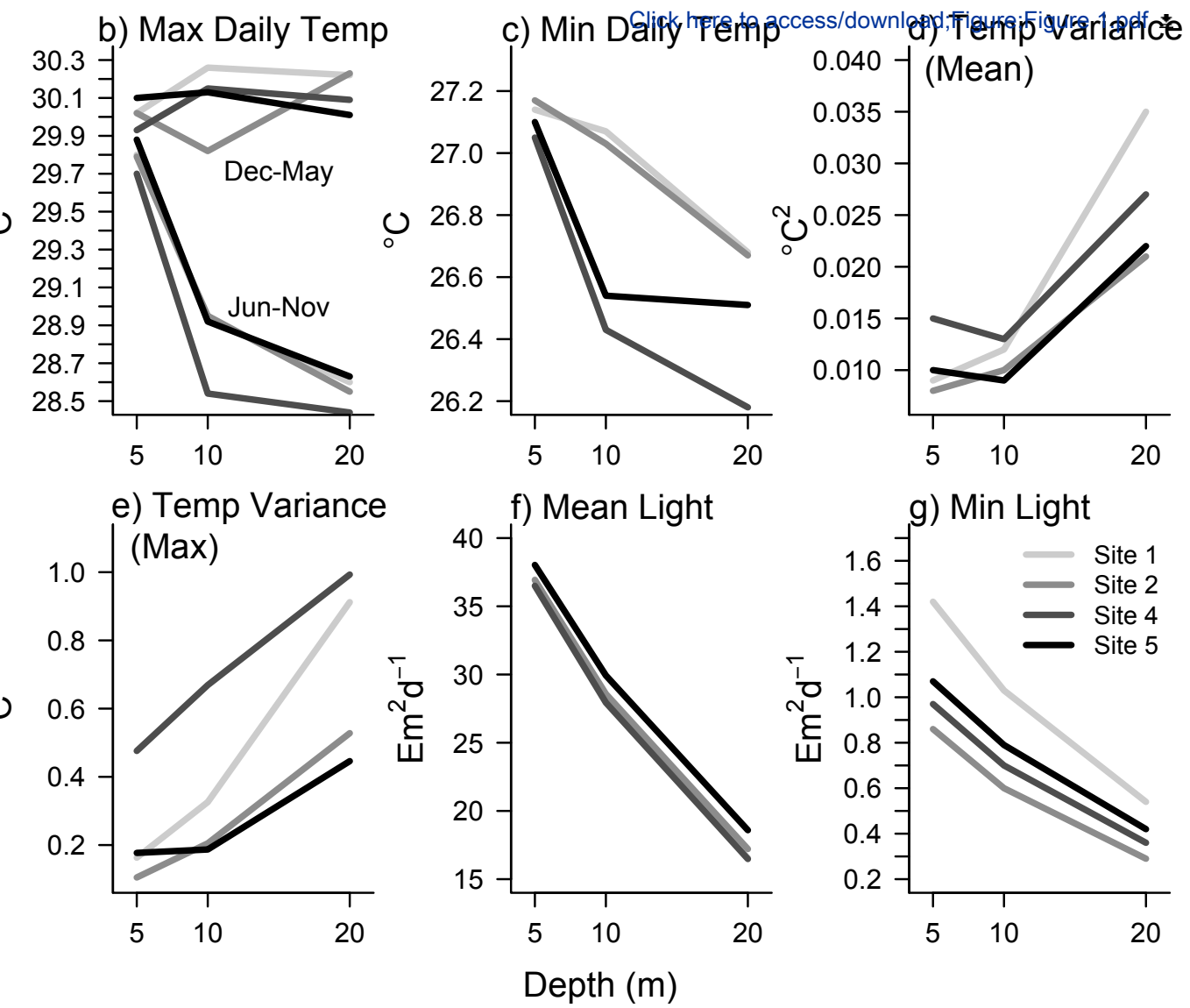
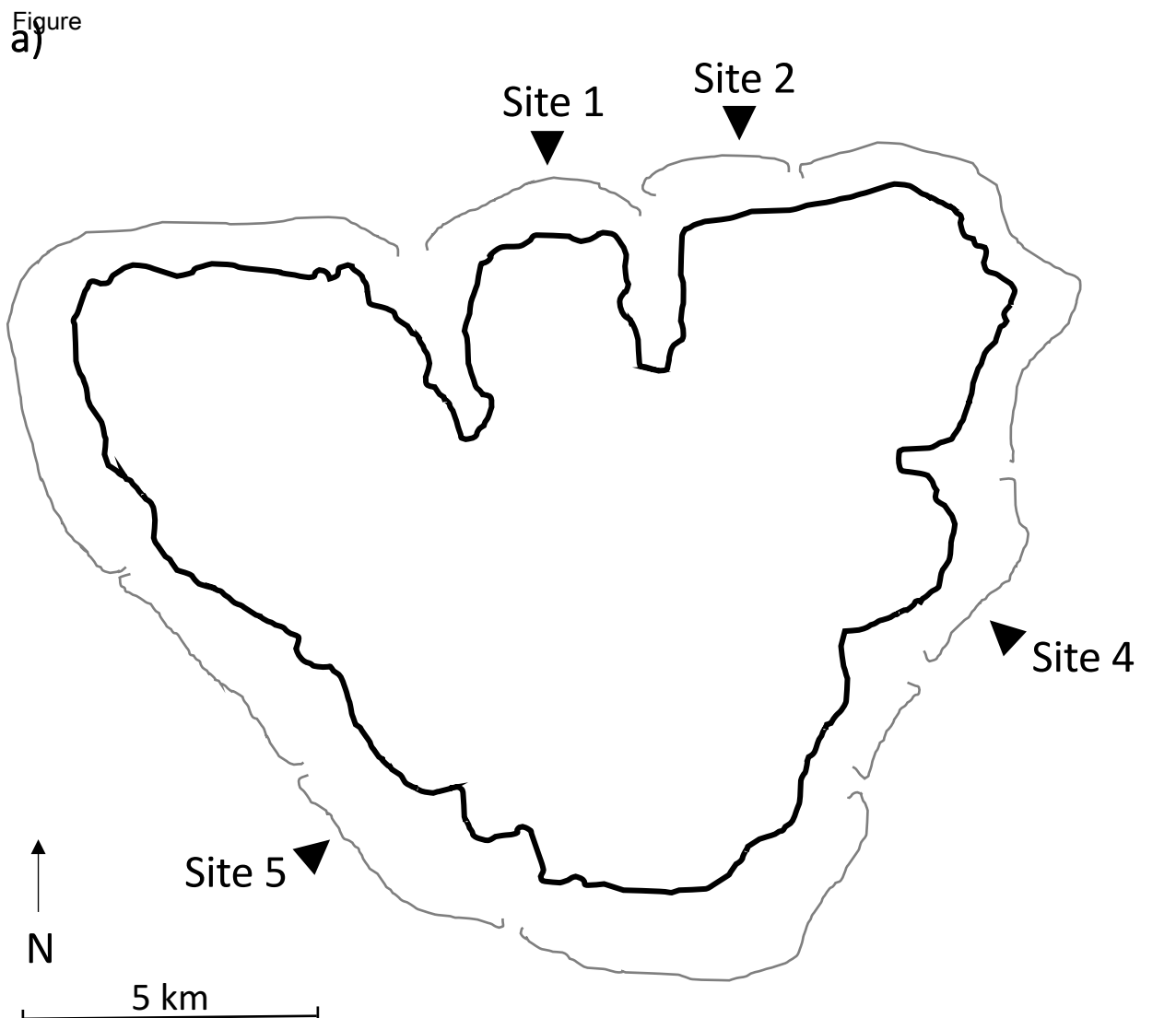
1
2
3
4 614 Richards ZT, Berry O, van Oppen MJH (2016) Cryptic genetic divergence within threatened
5 615 species of *Acropora* coral from the Indian and Pacific Oceans. *Conserv Genet* 1–15
6 616 Rocha LA, Robertson DR, Roman J, Bowen BW (2005) Ecological speciation in tropical reef
7 617 fishes. *Proc R Soc B Biol Sci* 272:573–579
8 618 Rouzé H, Lecellier G, Pochon X, Torda G, Berteaux-Lecellier V (2019) Unique quantitative
9 619 Symbiodiniaceae signature of coral colonies revealed through spatio-temporal survey in
10 620 Moorea. *Sci Rep* 9:
11 621 Sawall Y, Al-Sofyani A, Hohn S, Banguera-Hinestrosa E, Voolstra CR, Wahl M (2015)
12 622 Extensive phenotypic plasticity of a Red Sea coral over a strong latitudinal temperature
13 623 gradient suggests limited acclimatization potential to warming. *Sci Rep* 5:8940
14 624 Schmidt-Roach S, Lundgren P, Miller KJ, Gerlach G, Noreen AME, Andreakis N (2013)
15 625 Assessing hidden species diversity in the coral *Pocillopora damicornis* from Eastern
16 626 Australia. *Coral Reefs* 32:161–172
17 627 Schmidt-Roach S, Miller KJ, Lundgren P, Andreakis N (2014) With eyes wide open: a revision
18 628 of species within and closely related to the *Pocillopora damicornis* species complex
19 629 (Scleractinia; Pocilloporidae) using morphology and genetics. *Zool J Linn Soc* 170:1–33
20 630 Schmidt-Roach S, Miller KJ, Woolsey E, Gerlach G, Baird AH (2012) Broadcast spawning by
21 631 *Pocillopora* species on the Great Barrier Reef. *PLoS One* 7:e50847
22 632 Snyder RE, Chesson P (2004) How the spatial scales of dispersal, competition, and
23 633 environmental heterogeneity interact to affect coexistence. *Am Nat* 164:633–650
24 634 Souter P (2010) Hidden genetic diversity in a key model species of coral. *Mar Biol* 157:875–885
25 635 Todd PA (2008) Morphological plasticity in scleractinian corals. *Biol Rev* 83:315–337
26 636 Torda G, Lundgren P, Willis BL, van Oppen MJH (2013) Genetic assignment of recruits reveals
27 637 short- and long-distance larval dispersal in *Pocillopora damicornis* on the Great Barrier
28 638 Reef. *Mol Ecol* 22:5821–34
29 639 Tsounis G, Edmunds PJ (2016) The potential for self-seeding by the coral *Pocillopora* spp. in
30 640 Moorea, French Polynesia. *PeerJ* 4:e2544
31 641 Warner PA, Van Oppen MJH, Willis BL (2015) Unexpected cryptic species diversity in the
32 642 widespread coral *Seriatopora hystrix* masks spatial-genetic patterns of connectivity. *Mol*
33 643 *Ecol* 24:2993–3008
34 644 Whitney JL, Bowen BW, Karl SA (2018) Flickers of speciation: Sympatric colour morphs of the
35 645 arc-eye hawkfish, *Paracirrhites arcatus*, reveal key elements of divergence with gene flow.
36 646 *Mol Ecol* 27:1479–1493
37 647 Wyatt ASJ, Leichter JJ, Toth LT, Miyajima T, Aronson RB, Nagata T (2020) Heat accumulation
38 648 on coral reefs mitigated by internal waves. *Nat Geosci* 13:28–34
39 649 Yachi S, Loreau M (1999) Biodiversity and ecosystem productivity in a fluctuating environment:
40 650 the insurance hypothesis. *Proc Natl Acad Sci* 96:1463–8
41 651 Zhang DY, Lin K, Hanski I (2004) Coexistence of cryptic species. *Ecol Lett* 7:165–169
42 652 R Core Team (2019). R: A language and environment for statistical computing. R Foundation for
43 653 Statistical Computing, Vienna, Austria. <https://www.R-project.org/>.
44
45
46
47
48
49
50
51
52
53
54
55
56
57
58
59
60
61
62
63
64
65

1
2
3
4 655 **Figure 1:** a) Map of Mo'orea, French Polynesia (-17°32'S -149°50'W), showing location of sites
5 656 where *Pocillopora* samples and environmental data were collected. At each site, *Pocillopora*
6 657 samples were collected from 5 m, 10 m, and 20 m. b) - g) Summary of the environmental data
7 658 showing the relationship between environmental variables and depth at each site (shaded lines).
8 659 All data are for summer-time temperature (December to May) and light (December to February)
9 660 regimes, unless otherwise indicated.
10 661
11 662

12 663 **Figure 2:** Haplotype network of the mitochondrial ORF region (855 bp) for 673 *Pocillopora*
13 664 samples collected from the fore reef of Mo'orea, French Polynesia. Each black dot represents
14 665 one base pair difference. Species and haplotype identification follows Forsman et al. (2013),
15 666 Pinzón et al. (2013), and Schmidt-Roach et al. (2014). Haplotypes 3a, 3b, 3f, and 3h have been
16 667 identified as *P. verrucosa* (Schmidt-Roach et al. 2014). Haplotypes without a species name
17 668 associated with them have not been formally identified yet. The size of each circle represents the
18 669 relative abundance of each haplotype found at Mo'orea across four sites and three depths.
19 670
20 671

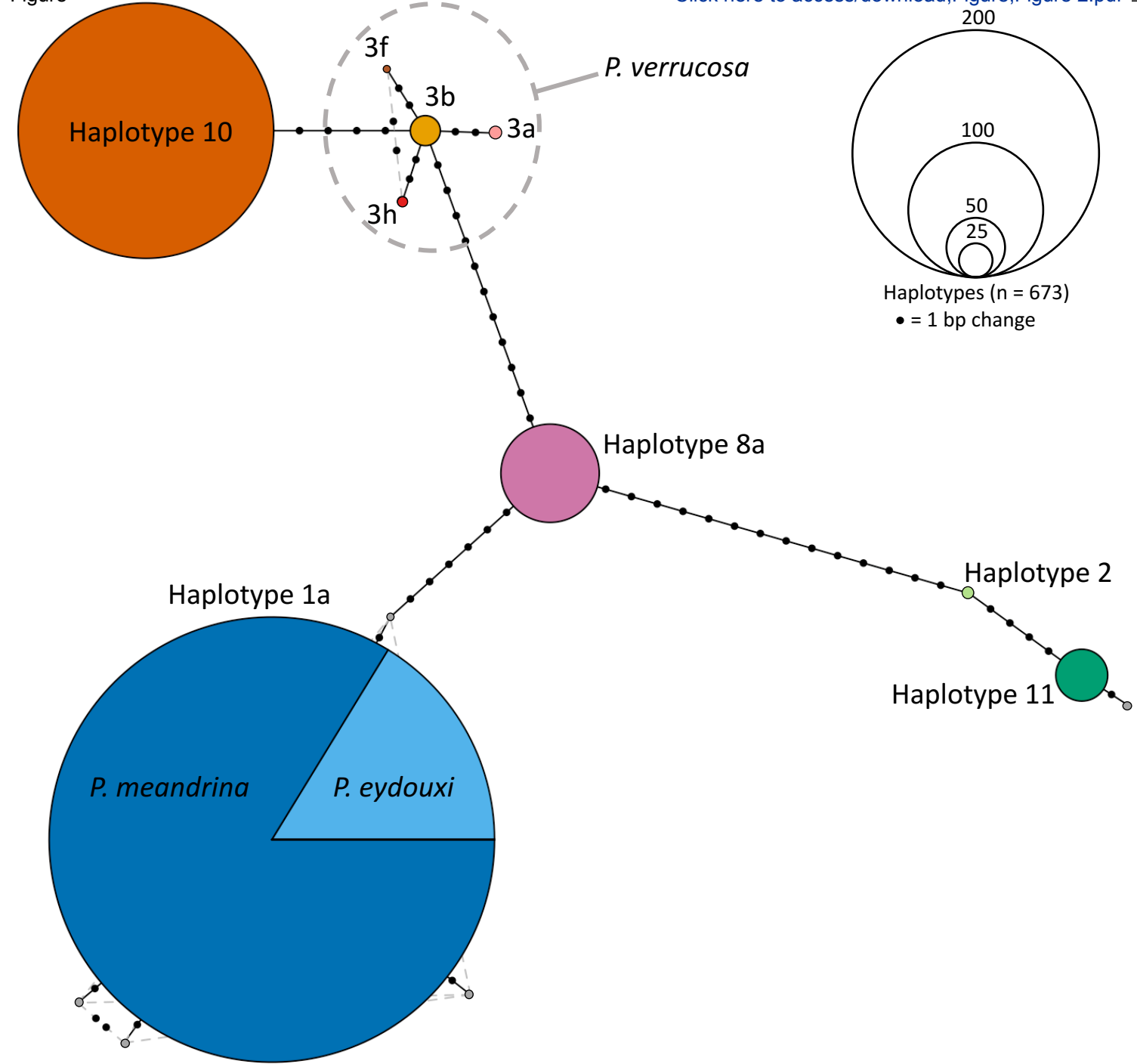
21 672 **Figure 3:** Proportion of *Pocillopora* species/haplotype (rows, examples provided on the right) at
22 673 5, 10, and 20 m depths at each site on the fore reef of Mo'orea in August 2019. Each bar denotes
23 674 the number of samples of that species divided by the total number of colonies sampled at that
24 675 depth and site. Black bars denote 95% confidence intervals based on the variance of a binomial
25 676 sampling distribution (i.e., $np(1-p)$, where n = number of samples, p = proportion). Values in
26 677 bold denote significant differences among depths at a given site for a given species. n indicates
27 678 the number of samples of that species at each depth.
28 679
29 680

30 681 **Figure 4:** Ordination biplot of the first two axes of the distance-based Redundancy Analysis (db-
31 682 RDA) using the environmental variables as the constraining variables. Sampling locations are
32 683 labelled by their site number in black. In a) species scores are plotted in blue, indicating the
33 684 relative contribution of each species in causing differences in the community composition among
34 685 sampling locations. Polygons group sites according to their depth. In b) arrows indicate biplot
35 686 scores for the environmental variables (constraining variables). Axis dbRDA1 explained 81.53%,
36 687 and axis dbRDA2 explained 5.62%, of the variation in the Bray-Curtis dissimilarity matrix. All
37 688 environmental data are for summer-time temperature (December to May) and light (December to
38 689 February) regimes, unless otherwise indicated.
39 690
40 691
41 692
42 693
43 694
44 695
45 696
46 697
47 698
48 699
49 700
50 701
51 702
52 703
53 704
54 705
55 706
56 707
57 708
58 709
59 710
60 711
61 712
62 713
63 714
64 715
65 716



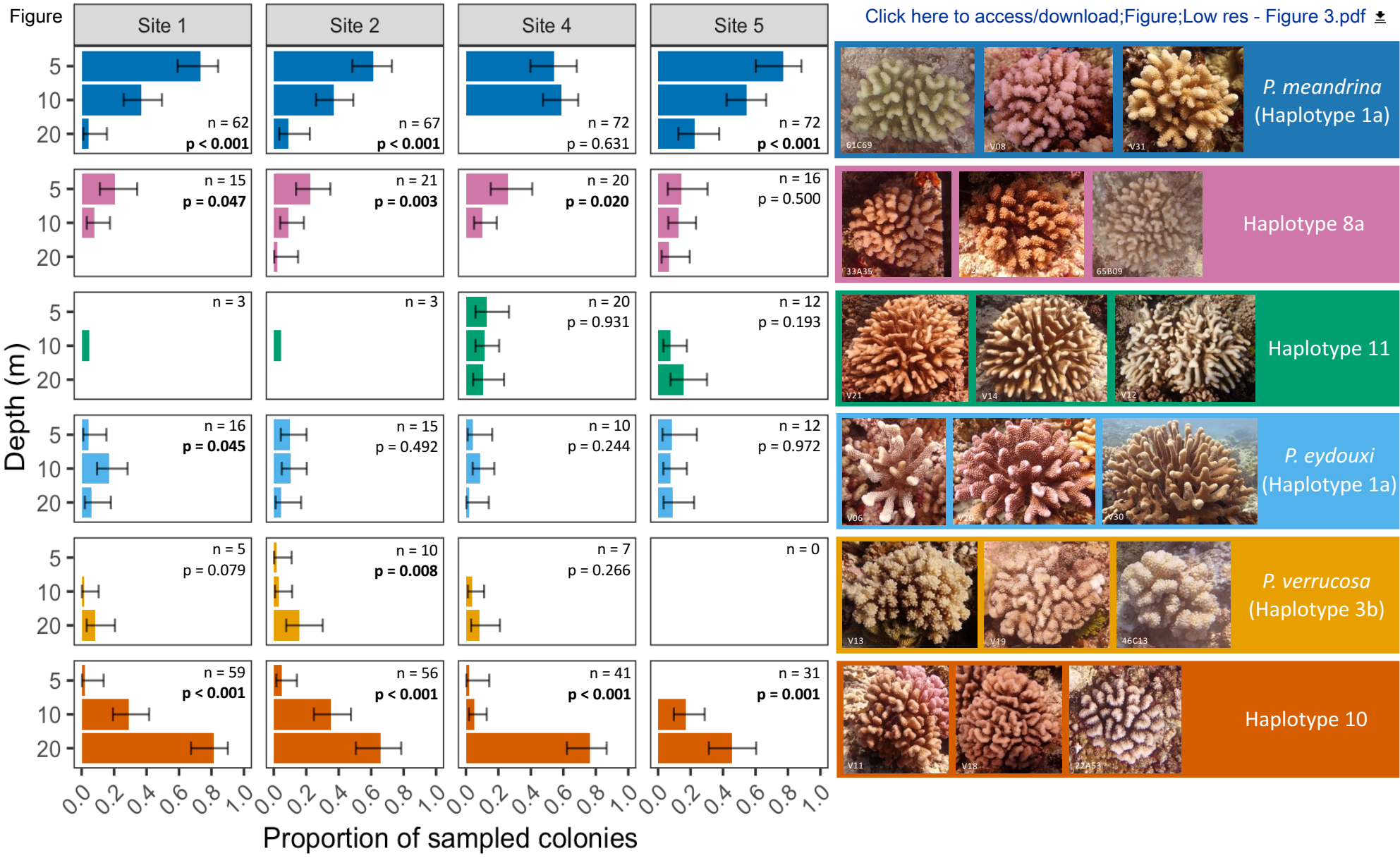
Figure

[Click here to access/download;Figure;Figure 2.pdf](#)



Figure

[Click here to access/download;Figure;Low res - Figure 3.pdf](#)



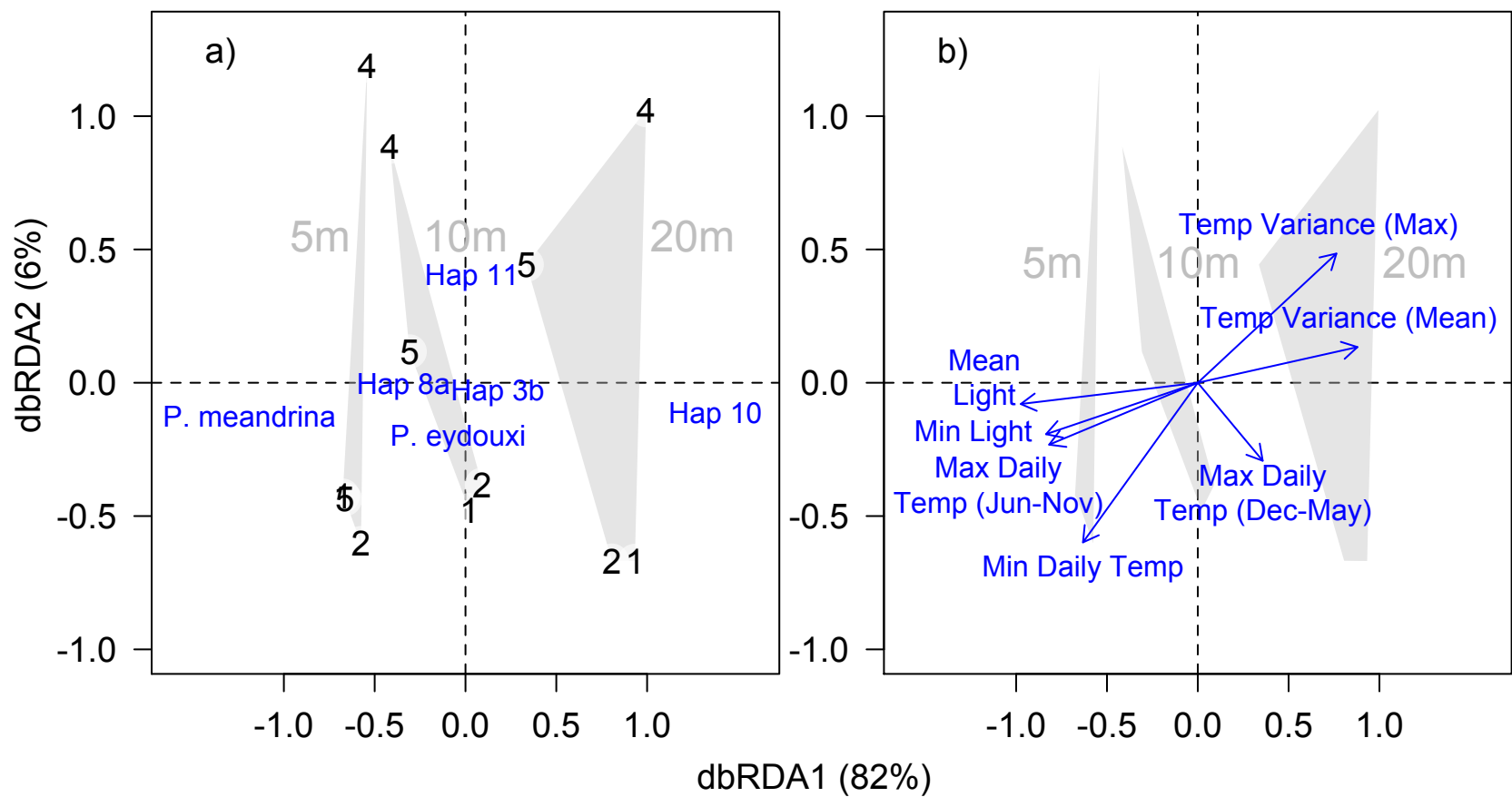


Table 1: Number of *Pocillopora* samples collected from each site at 5, 10, and 20 m depths.

Site	5 m depth	10 m depth	20 m depth
1	50	65	48
2	62	69	46
4	51	83	48
5	37	68	46

Table 2: ANOVA permutation test of the effect of depth (5, 10, and 20 m) and site (1, 2, 4, and 5), based on a distance-based Redundancy Analysis (db-RDA) using the environmental variables as the constraining variables. Tests of each factor are conditional on the presence of the other factor in the model (i.e., marginal tests). p-values are based on 9999 permutations.

	df	Sums of Squares	F-value	p-value
Depth	2	1.302	28.161	<0.01
Site	3	0.198	2.861	0.092
Residual	6	0.139		